The Nature of the Metal-Metal Bond in Bimetallic Surfaces

José A. Rodriguez and D. Wayne Goodman

The formation of a surface metal-metal bond can produce large perturbations in the electronic, chemical, and catalytic properties of a metal. Recent studies indicate that charge transfer is an important component in surface metal-metal bonds that involve dissimilar elements. The larger the charge transfer, the stronger the cohesive energy of the bimetallic bond. On a surface, the formation of a heteronuclear metal-metal bond induces a flow of electron density toward the element with the larger fraction of empty states in its valence band. This behavior is completely contrary to that observed in bulk alloys, indicating that the nature of a heteronuclear metal-metal bond depends strongly on the structural geometry of the bimetallic system.

In general, metals are elements characterized by the presence of a large number of valence orbitals that can donate or accept electrons. Isolated metal atoms are unstable, very reactive, and show a tendency to fully use all of their valence orbitals by making chemical bonds with other species. Thus, when two isolated metal centers are put in contact, they usually form a dinuclear compound in which the atoms can be united by a multiple metal-metal bond (*1*, *2*). In recent years, a large effort has been focused on understanding the chemical and physical properties of molecules and solids that have heteronuclear metal-metal bonds. In part, this interest has been motivated by the extensive technological applications that mixed-metal systems have in areas of metallurgy, catalysis, electrochemistry, and microelectronics fabrication. The two basic questions in these studies are: (i) What is the nature of the heteronuclear metal-metal bond? and (ii) How does the formation of this bond affect the physical and chemical properties of metals? The answer to these questions is a challenge to modern science and a prerequisite for a nonempirical design of bimetallic systems with industrial applications.

A large amount of experimental evidence (*3–5*) accumulated during the last 50 years for monometallic compounds indicates that in general the properties of a metal center depend on three factors: (i) the metal itself, (ii) the type of species bonded to the metal, and (iii) the geometrical structure of the system. In principle, one can expect that these factors can also influence the properties of a heteronuclear metal-metal bond. The next key question is which factor is dominant. For example, are the properties of the bond in a diatomic CuNi molecule identical to those of the bonds in a three-dimensional (3-D) CuNi alloy? In other words, is the nature of the metals much more important than the structural characteristics of the compound? Clearly, the answer to this question has a tremendous importance for understanding the properties of bimetallic surfaces, systems that can have 2-D periodicity and are intermediate between the isolated metal clusters studied by chemists and the 3-D metal alloys investigated by solid-state physicists. Indeed, results of photoelectron spectroscopy for monometallic solids indicate that the electronic properties of surface and bulk atoms are different (*6–9*). For solid metals, a reduction in the atomic coordination number produces a narrowing of the valence band at the surface. As a consequence, charge must flow between the surface atoms and the bulk so that the composite system maintains a common Fermi level (*6*, *8*, *10*). This phenomenon suggests that the properties of a bond in a bimetallic surface can be very different from those of the corresponding bond in a 3-D alloy, stressing the need to investigate the nature of the surface metal-metal bond.

In the study of surface metal-metal bonds, it has been advantageous to use model bimetallic systems generated by vapor depositing one metal onto a crystal face of a second metal (*11*, *12*). These well-defined bimetallic surfaces offer the possibility of correlating electronic and chemical properties of a system with atomic-level surface structure. In many cases, the results obtained by using well-defined bimetallic surfaces have revolutionized the way in which the surface metal-metal bond is viewed. This article summarizes the results of recent experiments in which the electronic and chemical properties of Ni, Pd, and Cu films supported on several transition-metal substrates have been investigated. Charge transfer appears to be an important component in surface metal-metal bonds that involve dissimilar elements. The larger the charge transfer, the stronger the cohesive energy of the bimetallic bond. A simple theory is developed that explains the nature of electron donor–electron acceptor interactions in noble- or transition-metal overlayers: Formation of surface metal-metal bonds leads to a gain in electrons by the element initially having the larger fraction of empty states in its valence band. This behavior, which is completely contrary to that seen in bulk alloys, is likely a result of the anisotropic character of a surface that changes the relative electronegativities of the metal atoms.

Surface Metal-Metal Bond: Cohesive Energy

In the last 10 years the properties of adlayers of Pd, Cu, or Ni on Ta(110) (*13–15*), Mo(110) (*16–19*), W(110) (*20–26*), Re(0001) (*27*, *28*), Ru(0001) (*17*, *29–34*), Rh(100) (*31*, *35*, *36*), and Pt(111) (*37–40*) have been the focus of considerable attention. At temperatures below 500 K, these bimetallic systems show no miscibility. The first monolayer of the admetal usually adopts a lattice constant that differs from its bulk crystal structure but that matches coherently the lattice of the underlying substrate (pseudomorphic growth). In general, but not always, only the first layer grows pseudomorphically, whereas subsequent layers tend to have lattice constants that are closer to the bulk crystal structure of the admetal.

The strength of the bonds between the metal overlayer and metal substrate can be probed directly by using thermal desorption mass spectroscopy (TDS). Representative TDS spectra for Cu and Pd films supported on Re(0001) are shown in Fig. 1 (*27*). The spectra are characterized by the presence of two peaks. The peak at higher temperature corresponds to desorption of the first layer of the admetal, and its position depends on the cohesive energy of the bimetallic bond. The peak at lower temperature is associated with desorption of multilayers of the film and is affected only by the strength of the

---

J. A. Rodriguez is in the Chemistry Department, Brookhaven National Laboratory, Upton, NY 11973. D. W. Goodman is in the Chemistry Department, Texas A&M University, College Station, TX 77843.

admetal-admetal bond. For submonolayer coverages of Pd, the spectra show a desorption temperature of ~1450 K. From this result, a dissociation energy of ~99 kcal/mol can be estimated for the Pd–Re(0001) bond (*27*). One monolayer of Cu shows a desorption maximum at ~1180 K. This value is considerably smaller than that for Pd, indicating that the Cu–Re(0001) bond is ~20 kcal/mol weaker than the Pd–Re(0001) bond. A similar trend is observed for several transition-metal substrates (*13–36*). In general, surface bonds involving a noble metal and a transition metal are much weaker than those in which both elements are transition metals.

For monometallic solids, bulk cohesive energies provide a useful scale to classify the strength of homonuclear metal-metal bonds (*41*). In a simple model, one can expect that these energies perhaps would be useful for predicting variations in the bond strength of different admetals on a given metal substrate (*41*). The basic idea is that the tendency of an element to form strong homonuclear metal-metal bonds should also be reflected in the strength of bimetallic bonds in which the element is involved (*41*). Experimental evidence indicates that this simple model is valid for overlayers of noble or first-row transition metals deposited on a fixed substrate (*41*). For example, noble metals on Ru(0001) show the following trend in admetal-substrate bond dissociation energies: Ag [67 kcal/mol (*42*)] < Cu [79 kcal/mol (*43*)] < Au [84 kcal/mol (*42*)]. This result is in qualitative agreement with the sequence observed for the bulk cohesive energies of Ag, Cu, and Au (*41*). In a similar way, desorption temperatures reported for monolayers of first-row transition metals on Ru(0001), Mn (*44*) < Cu (*30, 43*) < Ni (*29*), and on Mo(110) (*18*), Cu < Fe < Ni, also agree with trends found for cohesive energies of monometallic solids (*41*). However, the strength seen for the Pd–W(110) (*20*) and Pd–Ru(0001) (*28*) bonds cannot be explained by the cohesive energy of bulk Pd. The desorption temperature of submonolayer coverages of Pd on Ru(0001) [~1440 K (*28*)] is substantially higher than the corresponding value for Au overlayers [~1260 K (*42*)], but the bulk cohesive energies of these admetals are almost identical (*41*). Nickel has a bulk cohesive energy 13 kcal/mol greater than that of Pd (*41*). Nevertheless, results of TDS show that Pd forms bimetallic bonds on W(110) (*20*) and Ru(0001) (*28*) that are 4 to 6 kcal/mol stronger than those made by Ni (*22, 29*). Thus, Pd has an unexpected ability to make very strong bonds with other metal surfaces. More experimental data are necessary to verify if this result is typical of second-row transition metals or an anomaly of Pd. In any case, the type of interactions occurring in a bimetallic bond can be very different from those in a homonuclear metal-metal bond.

A comparison of the monolayer desorption temperature for Pd from Ta(110) (*13, 15*), W(110) (*20*), Re(0001) (*28*), and Ru(0001) (*28*) is shown in Fig. 2A. In going from a Ru to a Ta substrate, there is an increase of 100 K in the desorption temperature, which indicates an enhancement of ~7 kcal/mol in the strength of the Pd-substrate bond. The trend in Fig. 2A does not follow the sequence of bulk cohesive energies for the metal substrates (*41*): Ru << Re ≈ Ta < W. Instead, the TDS data indicate that the less occupied the valence *d*-band of the substrate, the stronger the Pd-substrate bond. Palladium has a valence band that is almost fully occupied. Therefore, electron donor–electron acceptor interactions between the adlayer and the substrate can be responsible for the trend seen in Fig. 2A.

The TDS results displayed in Fig. 3A for Ni monolayers on several substrates (*13, 18, 22, 29*) show the same general trend seen for Pd overlayers: The cohesive energy of the bimetallic bond increases as the

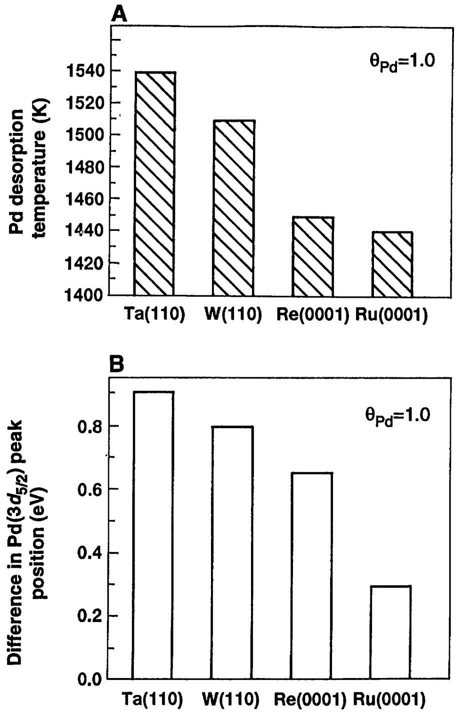

Fig. 2. (**A**) Desorption temperature of a Pd monolayer from several single-crystal substrates. (**B**) Difference in Pd($3d_{5/2}$) x-ray photoelectron (XPS) binding energy between one monolayer of Pd and the surface atoms of Pd(100) as a function of metal substrate. Data taken from (*13, 15, 20, 25, 27, 28*).

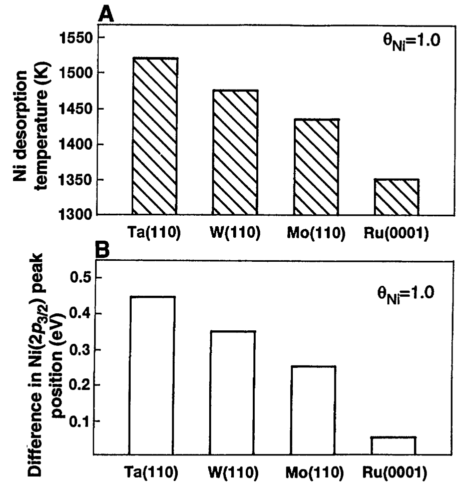

Fig. 3. (**A**) Desorption temperature for a monolayer of Ni from Ta(110) (*13*), W(110) (*22*), Mo(110) (*18*), and Ru(0001) (*29*). (**B**) Shifts in the Ni($2p_{3/2}$) XPS binding energy for a Ni monolayer on several substrates with respect to the surface atoms of Ni(100). Data taken from (*13, 17, 25*).

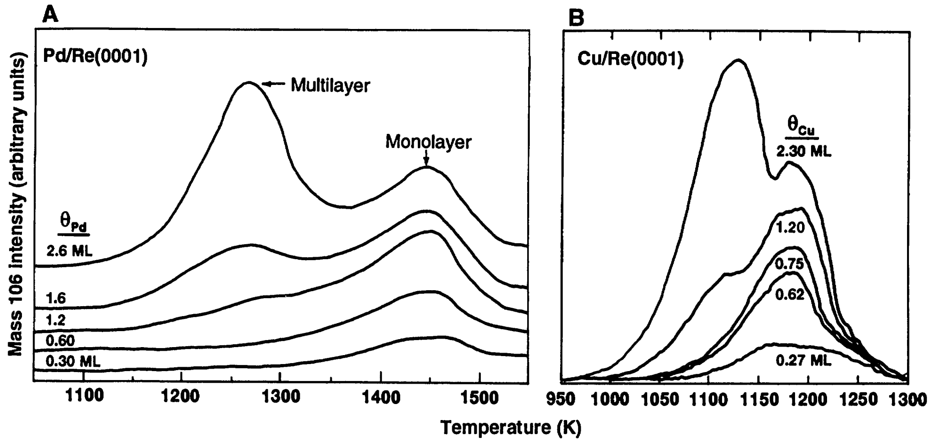

Fig. 1. Thermal desorption spectra for Pd and Cu films supported on Re(0001). The coverage of Pd, θ_{Pd}, or Cu, θ_{Cu}, is reported with respect to the number of surface atoms of Re(0001), with one adatom per substrate atom corresponding to $\theta = 1$ monolayer (ML). [Adapted from (*27*) with permission, © American Institute of Physics]

fraction of empty states in the valence band of the metal substrate increases. Interesting behavior is observed in Fig. 4A for Cu adlayers. The strongest Cu-substrate bonds occur for the substrates on the extreme left- and right-hand sides of the transition series, with a minimum in the Cu desorption temperature for the Cu/Re(0001) system. Copper has a 4*s*-band that is only half occupied and interacts strongly with metals in which the valence band is either nearly empty or almost full. This type of behavior suggests again that charge transfer between metals can play an important role in the cohesive energy of surface metal-metal bonds. In the sections below, we review studies of photoemission spectroscopy and CO chemisorption that show significant charge transfer in bimetallic bonds involving dissimilar elements.

The trends in Figs. 3A and 4A for Ni and Cu adlayers on second- or third-row transition-metal substrates cannot be explained by comparing the bulk cohesive energies of the substrates (*41*), although variations in the bulk cohesive energy of noble and first-row transition metals certainly can explain trends observed for Mn, Ni, Cu, Ag, and Au on Ru(0001) or Fe, Ni, and Cu on Mo(110) (see above). A possible cause for this discrepancy is a change in the structural geometry of the substrate in Figs. 2 to 4. The desorption temperature of Pd and Ni on W(100) is ~30 K higher than on W(110) (*20, 22*). A reduction in the surface atomic density of the substrate increases the strength of the admetal-substrate bond. Thus, variations in the bulk cohesive energy of the substrate could be overcome by changes in the surface atomic density. Indeed, the desorption temperatures in Figs. 2A and 3A increase when the atomic density of the substrate decreases: Re(0001) ≈ Ru(0001) < Mo(110) ≈ W(110) < Ta(110). This simple "rule," however, cannot explain why the desorption temperature of Cu on Rh(100) is somewhat higher than that on Ta(110), with Rh(100) having a larger surface atomic density and much lower bulk cohesive energy than Ta(110) (*41*). As discussed below, the Cu–Rh(100) bond is much more ionic than the Cu–Ta(110) bond. In general, the strength of a bimetallic bond depends on three factors: (i) the bulk cohesive energy of the isolated metals (which gives an indication of the tendency of the elements to form metal-metal bonds); (ii) the structural geometry of the system; and (iii) the degree of ionicity in the bond. In the next section we examine the relative importance of factor (iii).

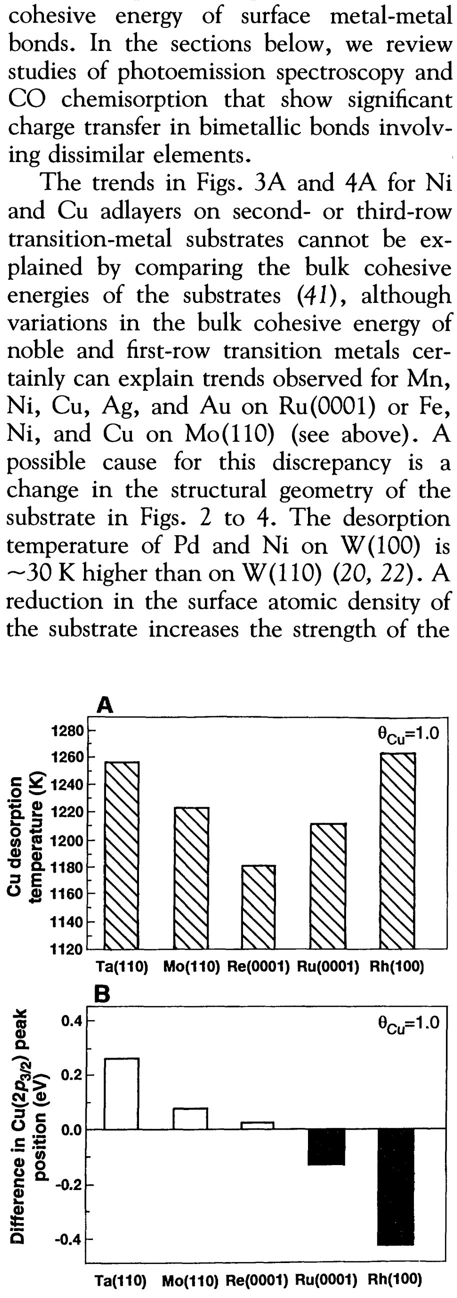

Fig. 4. (**A**) Desorption temperature of a Cu monolayer from several single-crystal substrates. (**B**) Difference in Cu($2p_{3/2}$) XPS binding energy between 1 ML of Cu and the surface atoms of Cu(100) as a function of metal substrate. Data taken from (*13, 16, 27, 30, 31, 35*).

Surface Bimetallic Bonds: Electronic Properties

X-ray and ultraviolet photoelectron spectroscopies (XPS and UPS) have been extensively used to investigate the core and valence levels of Ni, Cu, and Pd films supported on several transition-metal substrates (*13, 14, 16, 17, 25, 27, 28, 31, 32, 38, 45*). The results of these studies show quite clearly that formation of a heteronuclear metal-metal bond can induce large changes in the electron density of a metal. These modifications in electronic structure affect the cohesive energy of the bimetallic bond and the chemical properties of the metal.

Results of XPS and UPS for submonolayer Pd films supported on early transition metals show Pd(3*d*) core levels and Pd(4*d*) valence bands that are at higher binding energy than those corresponding to bulk Pd (*14, 16, 17, 27, 46*). This increase in binding energy is a consequence of charge transfer from the Pd adlayers to the metal substrates, which produces a reduction in electron-electron repulsion on the Pd atoms that stabilizes their core and valence levels (*16, 17, 28*). This interpretation is also consistent with results of work function measurements (*17, 21, 28, 47*) and CO adsorption (*16, 28*). How the difference in Pd($3d_{5/2}$) binding energy between a monolayer of supported Pd and the surface atoms of Pd(100) varies with metal substrate is shown in Fig. 2B. The magnitude of the charge transfer from Pd increases as the fraction of occupied states in the valence band of the substrate decreases. An identical trend is observed in work function measurements. On W(110), the decrease in work function induced by Pd adatoms is larger than that on Ru(0001) (*21, 28, 47*). A comparison of the XPS core-level shifts with the Pd desorption temperatures in Fig. 2 indicates that there is an excellent correlation between the two measurements. Systems that show the strongest Pd-substrate bonds also display the largest charge transfers between their elements.

The trends in core-level shifts and desorption temperatures displayed in Fig. 3 for supported Ni monolayers are similar to those found for the Pd overlayers. A notable difference between the behavior of these admetals is the magnitude of the electronic perturbations induced by bimetallic bonding. In all of these cases, the Pd-substrate bonds are more ionic than the Ni-substrate bonds. A similar result is seen in work function measurements for Pd and Ni on W(110) (*21, 23*). This difference cannot be explained in terms of atomic ionization potentials (*48*), which suggest that Ni should be a much better electron donor. One possible explanation for this difference between Ni and Pd is that the metallic radius of Pd (1.38 Å) is closer to that of the second- and third-row transition metal substrates than is the radius of Ni (1.25 Å). A good match in the overlayer-substrate radii for Pd results in an efficient overlap between the appropriate overlayer-substrate orbitals, which leads to a large charge transfer within the bond. The large degree of ionicity in the Pd-substrate bonds substantially affects their strength. On the basis of bulk cohesive energies (*41*), one would expect the bond of Ni on any metal substrate to be ~13 kcal/mol stronger than that of Pd. However, the fact that the Pd-substrate bonds are much more ionic than the Ni-substrate bonds makes the former 4 to 6 kcal/mol stronger than the later.

How the difference in Cu($2p_{3/2}$) binding energy between a monolayer of supported Cu and the surface atoms of Cu(100) depends on metal substrate is shown in Fig. 4B. The core-level shifts indicate that Cu transfers charge to early transition metals (Ta and Mo) and withdraws charge from late transition metals (Ru and Rh) (*16*). Copper has a 4*s* valence band that is half empty and can act as electron donor or electron acceptor depending on the relative fraction of empty states in the valence band of the substrate. For Re, the 5*d* valence band is also half empty; consequently, only a minor perturbation is observed for the Cu-Re system. Again, the systems that show the largest charge transfer between metals also show the strongest bimetallic bonds. The important role that charge transfer can play in the strength of a metal-metal bond is illustrated by the results for Cu/Ta(110) and Cu/Rh(100). The bulk cohesive energy of Ta is 54 kcal/mol greater than that of Rh (*41*), and the surface atomic density of Rh(100) is ~6% greater than that of Ta(110). These differences suggest that the Cu–Rh(100) bond should be much weaker than the Cu–Ta(110) bond. Nevertheless, the larger ionicity in the Cu–Rh(100) bond is the dominant factor, making this bond ~1 kcal/mol stronger than the Cu–Ta(110) bond.

In order to fully understand the trends observed in Figs. 2 to 4, it is necessary to have detailed quantum-mechanical information about the bonding mechanism between the Ni, Cu, or Pd overlayers and the metal substrates. Such information is not available at present. However, a simple model that explains the observed trends evolves by considering the type of metals present in the bimetallic surfaces (*16*). The largest transfer of electron density is found in systems that involve a combination of a metal with an almost fully occupied valence band and a metal with a valence band more than half empty. It appears that formation of a surface metal-metal bond generally leads to a gain in electron density by the element initially having the larger fraction of empty states in its valence band. Thus, early transition metals behave as electron acceptors, whereas late transition metals are electron donors. The direction of electron transfer on a surface can be easily understood in terms of orbital mixing (*16*): Hybridization of the occupied states of an electron-rich metal A with the unoccupied levels of an electron-poor metal B leads to a loss of A character in the occupied states and hence a reduction in the electron density on metal A. As discussed below, the direction of charge transfer found in a bimetallic surface can be very different from that seen in a 3-D alloy.

Chemical Properties of Bimetallic Systems: CO Adsorption

It can be expected that the electronic perturbations described above would modify the chemical properties of the metal overlayers. The results of many studies dealing with the chemisorption of CO on well-defined bimetallic surfaces indicate that indeed this is the case (*27, 49*). A correlation between changes in CO desorption temperature and relative shifts in surface core-level binding energies for supported monolayers of Pd, Ni, and Cu is shown in Fig. 5. Strong electron donor–electron acceptor interactions present in bimetallic bonding deactivate Pd and Ni adatoms toward CO chemisorption, whereas the same type of phenomena activate Cu adatoms. Bimetallic surfaces with the strongest Pd-substrate bonds have the weakest Pd–CO bonds. In contrast, surfaces with the strongest Cu-substrate bonds show also the strongest Cu–CO bonds.

For Pd on early transition metals, the Pd–CO bond is considerably weaker than that observed for Pd(100) (*13, 15, 20, 27*). The extreme case is CO/Pd/Ta(110), which shows a reduction of 235 K in the CO desorption temperature and a weakening of ~15 kcal/mol in the strength of the Pd–CO bond. According to the XPS and work function data discussed above, the electron density of supported monolayers of Pd is less than that of the surface atoms of Pd(100). A partial positive charge on the Pd adatoms is consistent with a reduction in their ability to coordinate CO through backdonation of electrons into the 2π orbitals, producing a weaker Pd–CO bond on the supported monolayers compared to Pd(100) (*16, 28*). Our model predicts that the electron density and ability to π-backdonate of the Pd surface atoms would follow the sequence: Pd/Ta(110) < Pd/W(110) < Pd/Ru(0001) < Pd(100). This trend is in excellent agreement with the TDS results in Fig. 5. A qualitative indication of the amount of π-backdonation in a Pd–CO bond can be obtained by measuring the shift in the Pd($3d_{5/2}$) XPS peak position induced by CO chemisorption (*28, 32*). This shift is ~1 eV smaller for CO/Pd/Ta(110) than for CO/Pd(100) (*13, 28*), indicating that π-backbonding toward CO is very weak on the Pd overlayer. The reduction of the electron population in the antibonding 2π orbitals of adsorbed CO is also reflected in results of vibrational spectroscopies (*13, 50*) that show a C–O stretching frequency for CO on Pd/Ta(110) at a much higher value than that observed on Pd(100).

In Fig. 5, Ni and Pd monolayers on early transition metals show similar behavior, but the decrease in CO desorption temperature is much less on the Ni adatoms. For Ni on W(110), the loss of electron density due to bimetallic bonding is considerably lower than for Pd (see above), and as a consequence there is only a slight weakening of the Ni–CO bond. The Ni/Ru(0001) system does not obey the correlation: The increase in core-level binding energy is not accompanied by a reduction in CO desorption temperature. In this surface, the charge transfer between metals is minimal because it combines two electron-rich elements. Thus, the Ni–Ru(0001) bond is mainly covalent, and the CO chemisorption ability of the metal adatoms cannot be predicted on the basis of charge transfer arguments (*17, 27*).

For monolayers of Cu deposited on electron-rich metals (Ru, Rh, and Pt), the XPS results suggest an enhancement in the electron density and π-backbonding capacity of the Cu adatoms with respect to the surface atoms of Cu(100). This result agrees well with TDS data that show larger (30 to 70 K) CO desorption temperatures from the supported Cu monolayers than from Cu(100) (*38, 39, 49*). Adsorption of CO on Cu films induces a large increase in the Cu($2p_{3/2}$) XPS binding energy, in part, due

Fig. 5. Correlation between shifts in surface core-level binding energy (from Figs. 2 to 4) (white bars) and shifts in CO desorption temperature (black bars). The properties of the Pd, Ni, and Cu monolayers are compared with the corresponding values for the (100) face of the pure metals. The Pd($3d_{5/2}$), Ni($2p_{3/2}$), and Cu($2p_{3/2}$) XPS peak positions were measured before adsorbing CO. [Reprinted from (*27*) with permission, © American Institute of Physics]

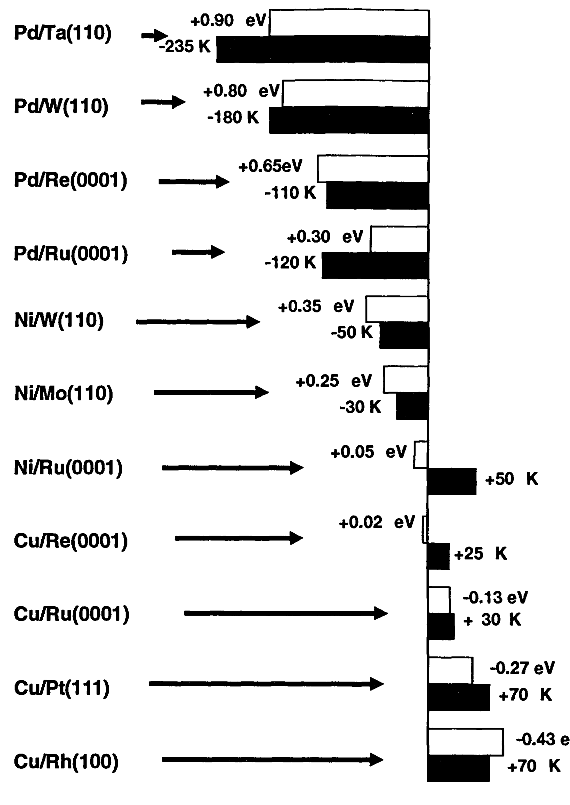

to π-backdonation (*16, 32*). How the CO-induced shift in Cu(2$p_{3/2}$) peak position (measured after saturating the surfaces with CO at 100 K) changes with metal substrate (*16, 40*) is shown in Fig. 6. A general trend can be observed: The strength of the Cu–CO bond, the amount of π-backdonation, and the C–O stretch frequency increase (or decrease) simultaneously. The Cu surfaces that are the best electron donors toward CO [Cu/Rh(100) and Cu/Pt(111)] also have the strongest Cu–CO bonds. However, they do not show the lowest C–O stretch frequencies, but the highest. For these systems, the variations in the vibrational frequency are not controlled by changes in the electron population of the CO(2π*) orbitals (*40*). Instead, the CO vibrational shifts arise from combining the following phenomena (*40*): (i) π-backdonation, (ii) the interaction between the CO dipole moment and the charge on the metal center, and (iii) the repulsion originating when the CO molecule stretches in the presence of the rigid surface to which it is bound (the so-called wall effect).

Fig. 6. Properties for CO adsorbed on pure monometallic surfaces like Cu(100), Cu(111), and Pt(111) are compared to the corresponding values for adsorption of the molecule on Cu monolayers pseudomorphic to Ru(0001), Rh(100), and Pt(111). Black bars, desorption temperature of CO; white bars, CO-induced shift in metal core level; and cross-hatched bars, CO stretching frequency. For Cu$_{1.0}$/Ru(0001), Cu$_{1.0}$/Rh(100), Cu$_{1.0}$/Pt(111), and Cu(100), the figure displays the shift in Cu(2$p_{3/2}$) core-level binding energy induced by CO adsorption. In the case of CO/Pt(111), the shift induced by CO upon the Pt(4$f_{7/2}$) level of the surface atoms is shown. The reference line represents 2050 cm^{-1}, 0.0 eV, and 150 K. [Reprinted from (*40*) with permission, © American Institute of Physics]

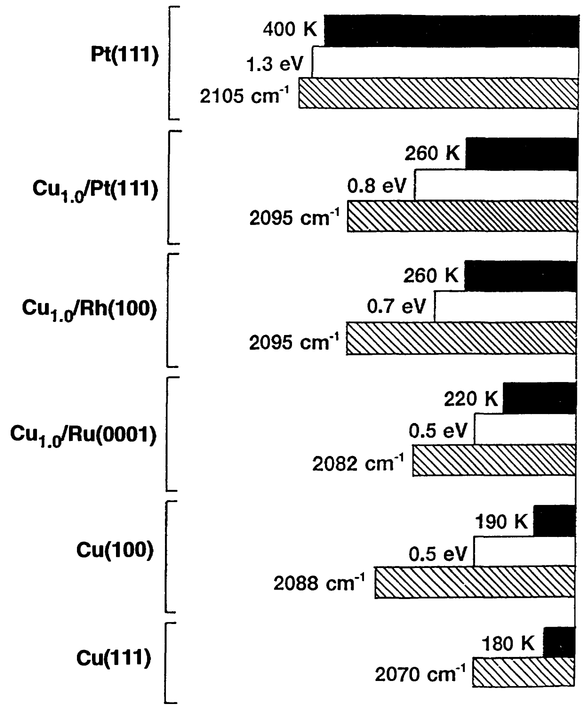

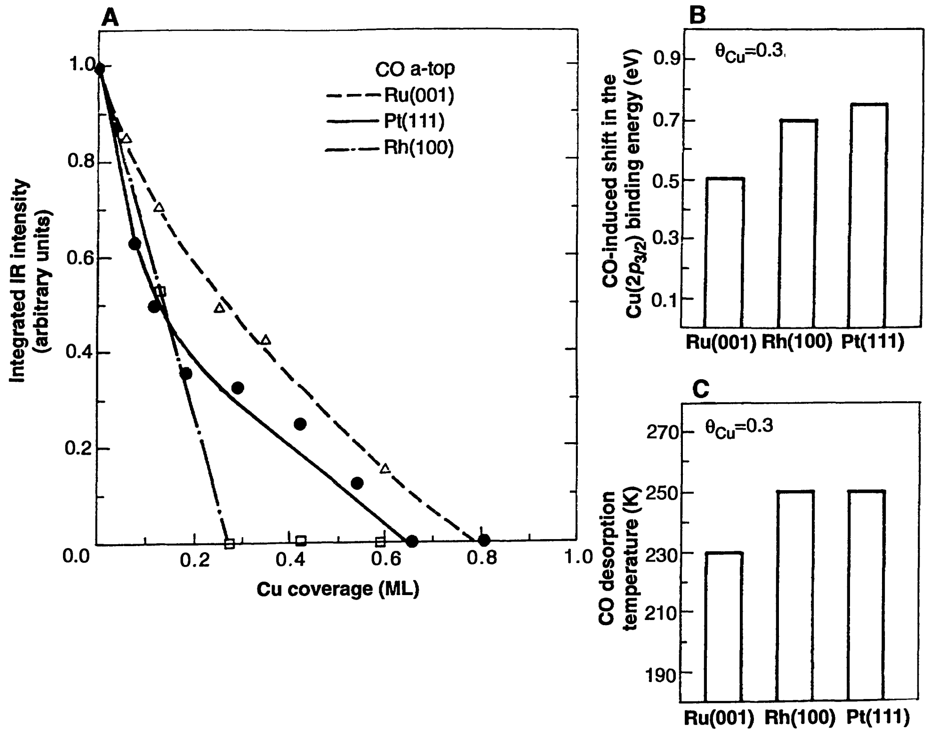

Fig. 7. (**A**) Effect of Cu coverage on the IR intensity for CO bonded to Ru, Rh, or Pt in Cu/Ru(0001), Cu/Rh(100), or Cu/Pt(111), respectively. The values correspond to surfaces saturated with CO at 85 to 100 K. (**B**) Shift in Cu(2$p_{3/2}$) binding energy induced by adsorption of CO on Ru(0001), Rh(100), and Pt(111) surfaces covered with 0.3 ML of Cu. (**C**) Desorption temperature of CO from Cu adatoms supported on Ru(0001), Rh(100), and Pt(111). [Reprinted from (*40*) with permission, © American Institute of Physics]

Studies with XPS and UPS indicate that metal atoms supported on a crystal face of a second metal have a very large polarizability. The charge density in the admetal can be easily modified by adsorbing electron-donor or electron-acceptor molecules (*32*). In general, adsorption of CO produces a reduction in the electron density of the metal adatoms. The charge distribution in the metal adatom–CO units can make CO molecules bonded to the metal substrate "invisible" in the infrared (IR) spectrum by "screening" their dynamical dipole moment (*40*). It appears that IR intensities of adsorbed CO are not representative of the relative composition of bimetallic surfaces (*40, 51*). How Cu-bonded CO attenuates the IR signal of CO bonded to Ru(0001) (*33*), Rh(100) (*36*), and Pt(111) (*40*) is shown in Fig. 7A. The data correspond to surfaces saturated with CO at ~100 K, with the molecules adsorbed on Cu and substrate atoms. Results of TDS and XPS indicate that Cu blocks CO adsorption on the substrates on a one-to-one basis, with CO bonding to Ru, Rh, or Pt being eliminated only at $\theta_{Cu} \geq 1$ monolayer (ML). This result is not seen in the IR data. In general, the "screening" of the IR signal is larger for Cu on Pt(111) and Rh(100) (*40*). This result correlates with the XPS and TDS data shown in Fig. 7, B and C. The larger the charge transfer from Cu to CO (π-backbonding), the stronger is the screening to the substrate-CO signal. The screening effect depends on the polarizability of the metal adatoms, which is controlled by the degree of ionicity in the bimetallic bond (*40, 51*).

Metal overlayers supported on single-crystal metal substrates can undergo phase transitions in which the 2-D structure of the surface changes as a function of temperature or admetal coverage (*11, 19, 24, 34, 52*). These phase transitions are frequently accompanied by variations in the electronic structure of the metal overlayer (*17, 19, 52*). The C–O stretch frequency in the IR spectrum is very sensitive to changes in the morphology of a metal overlayer (*24, 40*).

Disorder-order transitions of Ni, Cu, and Co films on several substrates (*24*, *33*, *36*, *40*) have been monitored with CO chemisorption and IR spectroscopy. Infrared spectra taken at 90 K after dosing CO to a Mo(110) surface covered with 1.29 ML of Ni (*24*) are shown in Fig. 8. The Ni was vapor deposited at 90 K and annealed briefly to the indicated temperatures before dosing CO. The spectrum of the unannealed Ni/Mo(110) surface shows peaks at 2097 and 2058 cm^{-1}. Annealing to higher temperatures increases the intensity of the 2058 cm^{-1} peak with its frequency shifted to 2068 cm^{-1}. This increase is at the expense of the intensity of the 2097 cm^{-1} peak. Low-energy electron diffraction experiments showed that deposition of Ni at 90 K produces a disordered overlayer, which transforms into an ordered (7 × 2) structure at temperatures above 500 K (*24*). The change in the morphology of the overlayer produces a reduction of ~ 30 cm^{-1} in the stretching frequency of adsorbed CO. A similar phenomenon has been observed for Cu overlayers on Ru(0001) (*33*), Rh(100) (*36*), and Pt(111) (*40*). The vibrational frequency of CO adsorbed on small Cu clusters is much higher (25 to 40 cm^{-1}) than that of CO bonded to well-ordered 2-D islands of Cu, which are pseudomorphic to the metal substrate. It is not completely clear what phenomena are responsible for this type of trend. One possible cause is an increase in the packing density of the metal adatoms during the phase transition (*40*).

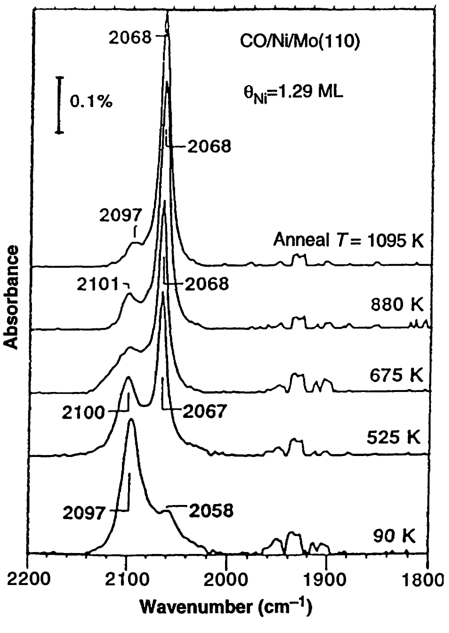

Fig. 8. Infrared spectra for CO adsorbed on 1.29 ML of Ni supported on Mo(110). The Ni overlayer was vapor deposited at 90 K, annealed to the indicated temperatures, and then saturated with CO at 90 K after each anneal. The IR spectra were collected at 90 K. [Reprinted from (*24*) with permission, © American Chemical Society]

Bimetallic Bonds and Surface Electronegativities

Electronegativity is a measure of the ability of a chemically bonded atom to attract electrons to itself (*53–55*). The studies discussed in the sections above indicate that charge transfer is an important component in surface metal-metal bonds that involve dissimilar elements. One may then ask what is the electronegativity of a metal atom on a surface, and how it differs from the electronegativity of metal centers in small compounds or 3-D alloys.

From a microscopic viewpoint, the electronegativity of an atom in a given compound depends upon the particular orbitals (pure or hybrid) that it uses for making bonds (*56–58*). In principle, variations in the coordination number of an atom or in the geometrical arrangement of its neighbors can produce changes in its orbital hybridization that modify its electronegativity (*55–58*). Thus, if we want to obtain a scale of electronegativities for metal adatoms, we must compare bimetallic systems that have similar coverage and structural geometry (*27*). The data in Figs. 2 to 4 can provide qualitative trends for surface electronegativities.

In many aspects, the behavior seen for the 2-D metal overlayers is different from that expected for bulk metals. Results of XPS (*25*), UPS (*46*), work function measurements (*21*, *23*), and CO chemisorption (*20*, *22*, *26*) for pseudomorphic monolayers of Ni and Pd on W(110) show that the surface electronegativity of Pd is much lower than that of Ni. This trend is contrary to that found in several scales of bulk electronegativities (*59*), where Pd is more electronegative than Ni. Data reported for monolayers of Ni, Cu, and Pd on Ru(0001) (*16*, *17*, *31*) also indicate a sequence of surface electronegativities (Pd < Ni < Cu) opposite to that found for bulk electronegativities (*59*). In different scales of electronegativity for bulk transition metals (*59*), the electronegativity increases from left to right in the periodic table. In 3-D metal alloys, charge is expected to flow from the element in the left to the element in the right of the periodic table (*59*). For example, experimental measurements and theoretical calculations for Pt alloys show net charge transfer from metals with low bulk electronegativity like Ta and W toward Pt (*60–62*). In contrast, the results presented above for Pd on Ta(110) and W(110) are consistent with charge transfer from Pd (an element with a relatively large bulk electronegativity) toward Ta and W (elements with low bulk electronegativity). Furthermore, the XPS and CO-TDS data indicate that the electronegativity of the substrate atoms in contact with the adlayers increases from right to left in the periodic table: Ta(110) > W(110) > Mo(110) > Re(0001) > Ru(0001) > Rh(100), contrary to trends seen in bulk electronegativities. If one takes into consideration that a surface atom is in an anisotropic environment that can produce large variations in electronegativity through orbital rehybridization (*55–58*), it is not surprising that the bulk and surface electronegativities of a metal are different.

The experimental evidence mentioned above indicates that the nature of a metal-metal bond in a bimetallic surface is very different from that of the corresponding bond in a bulk 3-D dimensional alloy. The properties of a heteronuclear metal-metal bond depend strongly on the structural geometry of the system. Transition and noble metals have a larger electronegativity than the alkali elements, but a much lower electronegativity than elements like Cl, S, and O (*48*). When a metal is bonded to a very electropositive or electronegative element, the direction of charge transfer within the bond is dominated by differences in the nature of the interacting species and the structural geometry of the system plays only a secondary role. For example, S and Cl withdraw electrons from metal atoms in inorganic compounds and on metal surfaces (*4*, *63–65*). In addition, alkali elements act as electron donors when bonded to metals in bulk alloys (*66*) or on surfaces (*64*, *67–69*). For these types of systems, the tendency of one of the elements to give or withdraw electrons is so large that it is impossible to modify the direction of charge transfer by altering the structure of the compound. In contrast, bimetallic systems involve species with similar electron donor–electron acceptor properties, and the subtle balance that determines the flow of charge between elements can be easily affected by changes in the coordination number or in the geometrical arrangement of the atoms.

Conclusions

A metal atom supported on a matrix of a dissimilar metal can be electronically perturbed, and this perturbation can dramatically alter the chemical properties of both constituents of the bimetallic system. Formation of a surface metal-metal bond produces a flow of electron density toward the element with the larger fraction of empty states in its valence band. This behavior is completely contrary to that observed in bulk alloys, indicating that the nature of a heteronuclear metal-metal bond depends strongly on the structural geometry of the system.

REFERENCES AND NOTES

1. F. A. Cotton and R. Walton, *Multiple Bonds Between Metal Atoms* (Wiley, New York, 1982).
2. *Symposium on Recent Advances in the Chemistry of Metal-Metal Multiple Bonds*, M. H. Chisholm, Ed., *Polyhedron* **6**, 665–801 (1987).
3. W. A. Harrison, *Electronic Structure and the Properties of Solids* (Freeman, San Francisco, 1980).
4. F. A. Cotton and G. Wilkinson, *Advanced Inorganic Chemistry* (Wiley, New York, ed. 5, 1988).
5. M. F. C. Ladd, *Structure and Bonding in Solid State Chemistry* (Horwood, Chichester, UK, 1979).
6. W. F. Egelhoff, *Surf. Sci. Rep.* **6**, 253 (1987).
7. P. H. Citrin and G. K. Wertheim, *Phys. Rev. B* **27**, 3176 (1983).
8. D. E. Eastman, F. J. Himpsel, J. F. van der Veen, *J. Vac. Sci. Technol.* **20**, 609 (1982).
9. K. G. Purcell, J. Jupille, D. A. King, *Surf. Sci.* **208**, 245 (1989).
10. A. Zangwill, *Physics at Surfaces* (Cambridge Univ. Press, New York, 1988), chap. 4.
11. C. T. Campbell, *Annu. Rev. Phys. Chem.* **41**, 775 (1990).
12. E. Bauer, in *The Chemical Physics of Solid Surfaces and Heterogeneous Catalysis*, D. A. King and D. P. Woodruff, Eds. (Elsevier, Amsterdam, 1984), vol. 3.
13. R. A. Campbell, W. K. Kuhn, D. W. Goodman, in preparation.
14. M. W. Ruckman, V. Murgai, M. Strongin, *Phys. Rev. B* **34**, 6759 (1986).
15. B. E. Koel, R. J. Smith, P. J. Berlowitz, *Surf. Sci.* **231**, 325 (1990).
16. J. A. Rodriguez, R. A. Campbell, D. W. Goodman, *J. Phys. Chem.* **95**, 5716 (1991).
17. R. A. Campbell, J. A. Rodriguez, D. W. Goodman, *Surf. Sci.* **256**, 272 (1991).
18. J.-W. He, W.-L. Shea, X. Jiang, D. W. Goodman, *J. Vac. Sci. Technol. A* **8**, 2435 (1990).
19. M. Tikhov and E. Bauer, *Surf. Sci.* **232**, 73 (1990).
20. P. J. Berlowitz and D. W. Goodman, *Langmuir* **4**, 1091 (1988).
21. W. Schlenk and E. Bauer, *Surf. Sci.* **93**, 9 (1980).
22. P. J. Berlowitz and D. W. Goodman, *ibid.* **187**, 463 (1987).
23. J. Kolaczkiewicz and E. Bauer, *ibid.* **144**, 495 (1984).
24. J.-W. He, W. K. Kuhn, D. W. Goodman, *J. Am. Chem. Soc.* **113**, 6416 (1991).
25. R. A. Campbell, J. A. Rodriguez, D. W. Goodman, *Surf. Sci.* **240**, 71 (1990).
26. Y. B. Zhao and R. Gomer, *ibid.* **239**, 189 (1990).
27. J. A. Rodriguez, R. A. Campbell, D. W. Goodman, *J. Vac. Sci. Technol. A*, in press.
28. R. A. Campbell, J. A. Rodriguez, D. W. Goodman, *Phys. Rev. B*, in press.
29. P. J. Berlowitz, J. E. Houston, J. M. White, D. W. Goodman, *Surf. Sci.* **205**, 1 (1988).
30. J. T. Yates, C. H. F. Peden, D. W. Goodman, *J. Catal.* **94**, 576 (1985).
31. J. A. Rodriguez, R. A. Campbell, D. W. Goodman, *J. Phys. Chem.* **95**, 2477 (1991).
32. J. A. Rodriguez, R. A. Campbell, J. S. Corneille, D. W. Goodman, *Chem. Phys. Lett.* **180**, 139 (1991).
33. F. M. Hoffmann and J. Paul, *J. Chem. Phys.* **86**, 2990 (1987); *ibid.* **87**, 1857 (1987).
34. G. O. Pötschke and R. J. Behm, *Phys. Rev. B* **44**, 1442 (1991).
35. X. Jiang and D. W. Goodman, *Surf. Sci.* **255**, 1 (1991).
36. J.-W. He, W. K. Kuhn, L.-W. H. Leung, D. W. Goodman, *J. Chem. Phys.* **93**, 7463 (1990).
37. R. C. Yeates and G. A. Somorjai, *Surf. Sci.* **134**, 729 (1983).
38. M. L. Shek, P. M. Stefan, I. Lindau, W. E. Spicer, *Phys. Rev. B* **27**, 7277 (1983); *ibid.* **27**, 7288 (1983).
39. M. T. Paffet, C. T. Campbell, T. N. Taylor, S. Srinivasan, *Surf. Sci.* **154**, 284 (1985).
40. J. A. Rodriguez, C. M. Truong, D. W. Goodman, *J. Chem. Phys.* **96**, 7814 (1992).
41. C. Kittel, *Introduction to Solid State Physics* (Wiley, New York, ed. 6, 1986), chap. 3; J. A. Rodriguez and J. Hbrek, unpublished results.
42. J. W. Niemantsverdriet, P. Dolle, K. Markert, K. Wandelt, *J. Vac. Sci. Technol. A* **5**, 875 (1987).
43. E. M. Stuve *et al.*, *Chem. Phys. Lett.* **149**, 557 (1988).
44. J. Hrbek, *J. Phys. Chem.* **94**, 1564 (1990).
45. J. E. Houston, C. H. F. Peden, P. J. Feibelman, D. R. Hamann, *Surf. Sci.* **192**, 457 (1987).
46. G. W. Graham, *J. Vac. Sci. Technol. A* **4**, 760 (1986).
47. C. Park, *Surf. Sci.* **203**, 395 (1988).
48. T. Moeller, *Inorganic Chemistry* (Wiley, New York, 1982), pp. 76—79 and 82–84.
49. J. A. Rodriguez, R. A. Campbell, D. W. Goodman, *J. Phys. Chem.* **94**, 6936 (1990).
50. A. Ortega, F. M. Hoffman, A. M. Bradshaw, *Surf. Sci.* **119**, 79 (1982).
51. J. A. Rodriguez, C. M. Truong, D. W. Goodman, *ibid.*, **271**, L331 (1992).
52. C. Kozioł, G. Lilienkamp, E. Bauer, *Phys. Rev. B* **41**, 3364 (1990).
53. L. Pauling, *The Nature of the Chemical Bond* (Cornell Univ. Press, Ithaca, NY, ed. 3, 1960).
54. R. T. Sanderson, *Chemical Bonds and Bond Energies* (Academic Press, New York, ed. 2, 1976).
55. L. H. Reed and L. C. Allen, *J. Phys. Chem.* **96**, 157 (1992).
56. J. Hinze and H. H. Jaffe, *J. Am. Chem. Soc.* **84**, 540 (1962).
57. ______, *Can. J. Chem.* **41**, 1315 (1963).
58. J. Hinze, M. A. Whitehead, H. H. Jaffe, *J. Am. Chem. Soc.* **85**, 148 (1963).
59. R. E. Watson and L. H. Bennett, *Phys. Rev. B* **18**, 6439 (1978).
60. R. E. Watson, L. J. Swartzendruber, L. H. Bennett, *ibid.* **24**, 6211 (1981).
61. R. E. Watson and L. H. Bennett, *Phys. Rev. Lett.* **43**, 1130 (1979).
62. R. E. Watson, J. W. Davenport, M. Weinert, *Phys. Rev. B* **35**, 508 (1987); *ibid.* **36**, 6396 (1987).
63. P. S. Bagus, G. Pacchioni, M. R. Philpott, *J. Chem. Phys.* **90**, 4287 (1989).
64. N. D. Lang, S. Holloway, J. K. Nørskov, *Surf. Sci.* **150**, 24 (1985).
65. D. W. Goodman, *Annu. Rev. Phys. Chem.* **37**, 425 (1986).
66. G. K. Wertheim, R. L. Cohen, G. Crecelius, K. W. West, J. H. Wernick, *Phys. Rev. B* **20**, 860 (1979).
67. H. P. Bonzel, *Surf. Sci. Rep.* **8**, 43 (1988).
68. J. A. Rodriguez, W. D. Clendening, C. T. Campbell, *J. Phys. Chem.* **93**, 5238 (1989).
69. G. A. Benesh and D. A. King, *Chem. Phys. Lett.* **191**, 315 (1992); G. Pacchioni and P. S. Bagus, *Surf. Sci.* **269/270**, 669 (1992).

70. Supported by the Department of Energy, Office of Basic Energy Sciences, Division of Chemical Sciences (grants to J.A.R. and D.W.G.), and the Robert A. Welch Foundation (grant to D.W.G.).

Genes, Patents, and Product Development

Rebecca S. Eisenberg

In the past year, the National Institutes of Health (NIH) has filed patent applications on more than 2750 partial complementary DNA sequences of unknown function. The rationale for the filings—that patent protection may be necessary to ensure that private firms are willing to invest in developing related products—rests on two premises: first, that NIH may obtain patent rights that will offer effective product monopolies to licensee firms, and second, that unless NIH obtains these rights now, firms will be unable to obtain a comparable degree of exclusivity by other means, such as by obtaining patents on their own subsequent innovations. Neither premise is clearly wrong, although both are subject to doubt in view of statements from industry representatives that the NIH patenting strategy will deter rather than promote product development.

Controversy about the impact of patent law on biomedical research is old news to observers of research science. In the 12 years since the U.S. Supreme Court upheld the patentability of genetically engineered organisms in *Diamond* v. *Chakrabarty* (*1*), the Patent and Trademark Office (PTO) has seen a deluge of patent applications covering biotechnology advances of every sort. So why are the recent patent applications on some 2750 partial cDNA sequences from the NIH laboratory of Dr. Craig Venter setting off alarm bells?

A telling distinction between the present controversy and that which erupted around the time of the *Diamond* v. *Chakrabarty* decision is that today it is the federal government that is pushing forward in pursuit of patent protection, while industry representatives are hesitating on the sidelines (*2*, *3*). And although some scientists are raising their voices in a now familiar refrain about the detrimental effects of patenting on scientific communications (*4*), the present controversy seems to be as much about the role of patents in promoting product development as it is about the role of patents in basic research. Opponents argue that the issuance of patents to those who randomly sequence partial cDNAs could undermine the incentives of firms to take up the more costly work of systematically finding genes of interest (*2*, *3*, *5*), whereas NIH asserts that patent protection at this stage may be necessary to ensure that private companies will be willing to develop products related to the partial genes (*6*).

For now, NIH characterizes the filings as an "interim policy" (*7*), *suggesting that it*

The author is a professor of law at the University of Michigan Law School, Ann Arbor, MI 48109.